Electrical conductivity study of porous carbons derived from rice husk

L. John Kennedy[1], J. Judith Vijaya[2], G. Sekaran[1*]

1. Department of Environmental Technology
Central Leather Research Institute, Adyar, Chennai, Tamil Nadu, India.

2. Department of Chemistry, Loyola Institute of Frontier Energy, Loyola College, Nungambakkam, Chennai,Tamil Nadu, India.

Abstract

The objective of this investigation was to evaluate the electrical conductivity of activated carbon derived from rice husk (RHAC) by two-stage process. DC conductivity measurements by two-probe method were determined for RHAC samples prepared at 700, 800 and 900^0C. The samples were compressed at a pressure of 75.9 kPa to 578.2kPa in a hollow glass cylinder using two metal plunges connected to a Keithley ammeter. The conductivity at room temperature was found to increase from $3.177x10^{-4}$ δ /cm to $1.99177x10^{-3}$ δ /cm for an increase in compression pressure. Dense packing of the material, collapse of pores and decrease in air gap between the carbon particles could be the factors for increase in conductivity with compression pressures. The temperature dependent conductivity of RHAC samples was determined by compressing the sample along with metal plungers and is followed by heating in a tubular heating furnace. A K-type thermocouple whose hot junction located in the close proximity of the specimen was used to monitor the temperature accurately. The specimen inside the furnace was heated by a microprocessor-controlled programmer up to 250^oC. The temperature dependent conductivity study conducted for the samples activated at 700, 800 and 900^0C had revealed that energy gap value of the samples were 0.1023ev, 0.0745ev and 0.052ev respectively, determined from the linear plot of ln I versus 1/T (K^{-1}). The meso porous RHAC samples were characterized using electron spin resonance, FT-IR spectroscopy and X-ray diffraction for quantitative evaluation of free electrons, functional groups and crystallites to support the mechanism of electrical conduction in mesoporous non-sinterable carbon samples.

1. Introduction

Porous carbon materials have attracted in these recent years much of interest as they are potential candidates for large number of applications especially in catalytic supports, battery electrodes, capacitors, gas storage and biomedical engineering [1-3]. As porous carbons are mostly amorphous in nature, a little presence of sp^2 carbon structures enhances the possibility of using these carbon materials for wider applications involving electrical conductivity [4,5]. The porous carbon materials contain sp^3 carbon fractions and a considerable sp^2 carbon fractions depending upon the preparation conditions and the raw material used. The sp^2 carbon sites in the carbon materials predominantly control the electronic and transport properties [6]. The properties of carbon materials with poor crystallinity have not been explored in detail yet, despite these carbons available to application in much higher quantities than graphite. Even though the chemical applications of these materials have been investigated in recant years, the exploitation of materials for physical and nonchemical application for little perhaps nil. This material has very interesting micro structures consist of the following [7] i) large density of the pores and defects, ii) dangling bonds particularly in the regions between the graphitic crystallites, iii) a large fractions of the carbons as surface atoms and iv) disordered crystallites. Because of these complexities it requires variety of experimental techniques to characterize both the surface and bulk properties. Hence we have included in one of the techniques to investigate the micro structure for which the electrical properties of rice husk based porous carbon has been considered in our investigations. Rice husk based porous carbon composite material was prepared contains carbon and SiO_2 as components of the material. SiO_2 being a known insulator, the conduction property of RHAC is assumed to be due to carbon component of the material. Hence our study was focused on the evaluation of conduction mechanism of carbon component of the composite material.

2. Experimental

The porous carbon composites were prepared in the laboratory by two-stage process using rice husk as the precursor material by chemical activation method [8]. The samples

treated at three different temperatures 700, 800 and 900°C and were labeled C700, C800 and C900 respectively.

2.1 Electrical conductivity studies

The dc electrical conductivity σ was measured at room temperature by the two-probe method. 1g porous carbon dried at 100°C over night was compressed in a hollow Pyrex glass cylinder with an inner diameter of 10 mm between two metal plungers at compression pressures ranging from 75.9 kPa to 578.2 kPa. The top and the bottom of the plungers are copper made and connected to a Keithley 2000 digital multimeter to measure the electrical conductivity of the samples.

2.2 Temperature dependence conductivity

In order to study the temperature dependent conductivity the whole set up i.e. the sample of a known weight compressed along with the two metal plungers kept inside a tubular heating furnace. A K type thermocouple whose hot junction located in the close proximity of the specimen was used to monitor the temperature accurately. The specimen inside the furnace was heated by a microprocessor-controlled programmer up to 250°C.

2.3 X-ray diffraction studies

X-ray diffraction experiments were performed with a Phillips X-pert diffractometer for 2θ values from 10 to 80° using CuKα radiation at a wavelength of λ = 1.540 A°. The other experimental conditions included 1/2° divergence slits, a 5-sec residence time at each step and intensity measurements in counts.

2.4 FT-IR studies.

A Perkin Elmer infrared spectrometer was used for the investigation of the surface function groups of the porous carbon. The carbon samples were mixed with KBr of spectroscopic grade and made into pellets at a pressure of about 1 MPa. The pellets were about 10 mm in diameter and 1 mm in thickness. The samples were scanned in the spectral range of 4000 – 400 cm^{-1}.

2.5 ESR measurements.

In the ESR measurements, Bruker IFS spectrometer was used to obtain the ESR spectrum. A small amount of carbon was loaded in the quarts tube. Vacuum was applied to remove the air from the carbon surface. An X-band microwave with a power of 1 mW and frequency of 9.771 GHz was applied to the specimen and recorded at room temperature.

3. Results and Discussion

3.1 Electrical Conductivity studies

The conduction was ohmic in nature and the electrical conductivity was given by [9]

$$\sigma = \frac{L}{R.A}$$

where R is the resistance (Ω), A is the area of the sample (cm^2) and L is the sample height (cm). The ohmic conduction at room temperature of carbon samples C700, C800 and C900 at compression pressure at 75.9 kPa were 8.02×10^{-5}, 1.5×10^{-4} and 3.28×10^{-4} δ/cm respectively. The conductivity contributed by the silica component can be assumed to be negligible as it is a good insulator and electrical conductivity by the sample is fully assumed to be due to carbon matrix. The electrical conductivity of the sample is assumed to be controlled by compression pressure as shown in Table1. We indeed obtained a six fold increase for rise in compression pressure from 75.9 to 578.2 kPa is σ approximately 3.288×10^{-4} and 2.025×10^{-3} δ /cm respectively for the sample C900 suggesting that sp^2 carbon structures must be separated to allow any conduction path between these regions [10]. Upon compression the individual particles in the composite material will be breaking, refolding into more dense packing and closer contacts between different particles will be created thereby increasing the electrical conductivity [11]. It is evident form the Table 1 that the electrical conductivity at 75.9kPa is low indicating the applied pressure is not sufficient to squeeze the pores or the air gap between the carbon particles. Hence inter particle electronic conduction becomes difficult. But the electrical conductivity increased by six fold at 578.2 kPa. It is due to the easy movement of electrons from one particle to another facilitated by the elimination of the air gap or porosity of the carbon by applying high pressure of compression.

These materials also seem to influence the high temperature activation energy of the conductivity measured in the temperature range of 30-250^{0}C. The energy gap is reproducible for the samples in the temperature range 30-250^{0}C were obtained using the expression [12] $I = I_o e^{-Eg/kT}$ where I is the current, E_g the energy gap, k the Boltzmann constant and T the temperature. Since $\ln I = \ln I_o - E_g/kT$, the plot of lnI vs 1/T gives linear curve. The energy gap value was calculated from the slope ($-E_g/k$). The carbon samples C700, C800, C900 exhibited increase in conductivity with increase in temperature, a characteristic feature of semiconductor. The observed E_g values for the composite samples C700, C800 and C900 were 0.123, 0.0745 and 0.0552 eV respectively. The plot of ln I vs the inverse of temperature indicates that the high temperature conduction process is thermally activated [10] with an associated activation energy. The plot of ln I vs 1/T shown in Fig.1 has two linear portions with small activation energy values thus exhibiting extrinsic semiconductor behavior. According to Robert and Schmidlen [13] the activation energy for electrical conduction in extrinsic semiconductors relates to the promotion of charge carriers from the dominant levels to the corresponding transport bands. Hence it is understood that the promotion of majority carriers takes place between the intermediate trap levels created due to impurities and interstitials as a result the composites have a lower energy gap values. The band gap width must be functions of carbonized temperature as shown in Fig. 2. It is also noted that these values of E_g are quite different from those deduced from the optical gap E_o of approximately 1.5 eV for all the three carbon samples which is related to π - π^* transitions of the centers of gaussian π - π^* bands. The variation of dc conductivity vs. inverse of the temperatures in the intermediate temperature range, 80 – 150^{0}C, lnI has a $T^{1/4}$ dependence clearly as shown in Fig.3 indicating that the conduction process is rather controlled by a variable range hopping process of the charge carriers within the band edges in agreement with Mott model for disordered or amorphous carbons [14]. The conductivity of amorphous semiconductors is influenced by the presence of dangling bonds (unsaturated bonds) which give rise to mid gap states in the band gap of the amorphous semiconductors [15].

The low values of E_g compared to E_o suggest that the electronic transport process is due to the transition between the localized defect band (π-π^*) states around the Fermi level. In our case the defect bands are assumed to have Gaussian distribution [10]. The

relatively low E_g value observed for C900 suggests a larger overlapping of the Gaussian π - π^* bands near the Fermi level as a result of higher density of defects in the case of these carbon materials. This defect density must also influence the optical gap E_o which is related to transition between the centers of Gaussian π - π^* band states. The higher values of E_o (1.5eV) compared to those of E_σ (0.0522 – 0.1023 eV) indicate that in the latter case the defects concerned by this process are rather located within the π band edges around the Fermi level [16]. The energy gap decreases upon increase in heat treatment of the carbon materials suggest a higher overlapping of the localized π band states in the vicinity of E_F as the proportion of the sp^2 carbon sites increase with temperature [17].

Table 1.
Room temperature conductivities and resistivities of for C900 at various pressures.

S. No	**Compression pressure kPa**	**Room temp conductivity (δ/cm)**	**Room temp resistivity (Ω cm)**
1	75.9	3.288×10^{-4}	3.041×10^{3}
2	230.9	8.127×10^{-4}	1.230×10^{3}
3	437.83	1.458×10^{-3}	6.86×10^{2}
4	578.2	2.025×10^{-3}	4.937×10^{2}

3.2 X-ray diffraction studies

The X-ray diffraction of the carbon sample C900 shown in Fig. 4 contains a mixture of amorphous and crystalline phases of silica. The peak corresponds to $2\theta = 21°$ and $2\theta = 24°$ are identified as crystobalite and tridymite [18]. In addition a sharp peak was observed at $2\theta = 26°$ and a very small one was at $2\theta = 44°$ indicating the slight formation of the (002) and (100/101) planes respectively of the graphitic structure. The temperature employed for activation of the precursor material can be sited as the reason for the formation of the small graphitic structures and for the crystallization of silica. The X-ray diffraction studies were not helpful in detecting the mechanism of electronic conduction. This is probably because these characterization techniques reflect the overall structure of

the specimens and are not sensitive to a partial structural change such as rearrangement, due to charge carrier transport.

3.3 FT-IR studies

The infrared spectroscopic data in Fig. 5 provides information on the chemical structure of activated carbon samples. All the carbon samples show a wide band at about 3250 – 3425 cm^{-1} due to O-H stretching mode of hexagonal groups and adsorbed water. The position and asymmetry of this band at lower wave numbers indicate the presence of strong hydrogen bonds [19]. The samples C700, C800 and C900 show absorption bands due to aliphatic C-H at 2920 cm^{-1}. A very small peak near 1700 cm^{-1} is assigned to C=O stretching vibrations of ketones, aldehydes, lactones or carboxyl groups. The weak intensity of this peak for all the carbons indicates porous carbons contain a small amount of carboxyl group. The broad peak shouldered a about 1115 cm^{-1} and sharp peaks at 805 and 475 cm^{-1} in the carbon samples indicate the presence of silica [20].

3.4 ESR spectra

Fig.6 shows the ESR spectra of the carbon C900. The ESR signal is due to the appearance of unpaired electrons during its formation [21]. The g-factor calculated is about 2.0083. Activated carbons are an ideal material for ESR measurements because of a high density of localized spins is expected due to their specific structure where a high ratio of surface atoms with localized spin exist. The spectra is broad indicating a fast interaction of existing spins. It is also noted that the broadening of the ESR spectrum occurs due to a fast energy transfer from a localized spin to another spin or to the lattice [22]. In other words, charge carriers can move fast. These kind of carbons have large ratio of surface atoms with dangling bonds where the localized spin exists. The energy level of these localized electrons should be similar to that of the electrons in a free atom and thus the energy levels resulting from those localized electrons appear between the bonding levels and antibonding levels (π - π^*). Hence the high density of these extra levels play a important role in the transport properties because the energy gap between the electronic states is very small due to the high density of states (DOS), the excitation

of the localized carriers becomes so easy that a quite high conductivity is observed at normal and high temperatures.

4. Conclusion

The electron transport properties of the carbons prepared are investigated in detail with their microstructure. The electrical conductivity, ESR and FTIR techniques were carried out to fully characterize the carbon materials. The analysis of the variation of conduction as a function of temperature showed two different conduction process operating respectively at moderate temperatures $T < 150°C$ and high temperatures $150 < T < 250°C$. The first process due to a variable range hopping mechanism in the π localized states around E_F following Motts law and the second one is thermally activated associated with energy gap of 0.0522 – 0.1023 eV for the three carbons. The ESR signal of the carbons C900 is due to the defects associated with broken bonds located on carbon sites. The presence of the graphitic structure has been confirmed from the X-ray diffraction pattern the sample. The surface function groups of the different carbons were discussed.

Acknowledgement

The work was supported by the Council of scientific and industrial research (CSIR) of India by providing financial assistance through senior research fellowship, provided to the first author.

References

[1] Hamdy Farag, White hurst DD, Isao Mochida. Synthesis of active hydrosulfurization carbon supported Co-Mo catalysts. Relationship between preparation methods and activity/selectivity. Ind Eng Chem Res 1998; 37: 3533-9.

[2] Quinn DF, Ragan S. Carbon suitable for medium pressure (6.9MPa) methane storage. Adsorp Sci Tech 2000; 18 (6): 515-27.

[3] Elzbieta Frackowiak, Francois Beguin. Carbon materials for the electrochemical storage of energy in capacitors. Carbon 2001; 39: 937-50.

[4] Robertson J. Hard amorphous (diamond- like carbons). Prog Solid State Chem 1991; 21: 199 – 333.

[5] Fusco G, Tagliaferro A, Milne WI, Robertson J. Diamond Relat Mater 1997; 6: 783- 786.

[6] Chhowala M, Robertson J, Chen CW et al. Influence of ion energy and substrate temperature on the optical and electronic properties of tetrahedral amorphous carbon. J Appl Phys 1997; 81: 139-145.

[7] Manivannan A, Chirila M, Giles MC, Seetra MS. Microstructure, dangling bonds and impurities in activated carbons. Carbon 1999; 37: 1741-7.

[8] Kennedy LJ, Vijaya JJ, Sekaran G. Effect of two stage process on the preparation and characterization of porous carbon composite from rice husk by phosphoric acid activation. Indus Eng Chem Res 2004; 43: 1832 - 1838.

[9] Dana Pantea, Hans Darmstadt, Serge Kaliaguine, Lyelia Summchen, Christian Roy. Electrical conductivity of thermal blacks. Influence of surface chemistry. Carbon 2001; 39: 1147-58.

[10] Racine B, Benlahsen M, Zellama K, Bouzerrar R, Kleider JP, Von Bardeleben JP et al. Electronic properties of hydrogenated amorphous carbon film deposited using ECR-RF plasma method. Diamond Relat Mater 2001; 10: 200-6.

[11] Mrozowski S. studies of carbon powders under compression I. Third Biennial Carbon Conference 1958; 495-508.

[12] William Smith F. Electrical properties of Materials. Foundations of Materials Science and Engineering. 2nd ed. Mc Graw-Hill Publication. 713-72.

[13] Roberts GG, Schmidlin FW. Study of localized levels in semi-insulators by

combined measurements of thermally activated ohmic and space – charge limited conduction. Phys Rev 1969; 180: 785-94.

[14] Daud WM, Badri M, Mansor H. Possible conduction mechanism in coconut – shell activated carbon. J Appl Phys 1990; 67(4): 1915-7.

[15] Jen Cordelair, Peter Greil. Electrical conductivity measurements as a microprobe for structure transitions in polysiloxane derived Si-O-C ceramics. J Euro Ceram Soc 2000; 20: 1947-57.

[16] Palinginis KC, Lubianiker Y, Cohen JD, Illie A, Kleinsorge B, Milne WI. Defect densities in tetrahedrally bonded amorphous carbon deduced by junctions capacitance techniques. Appl Phys Lett 1999; 74(3): 371-3.

[17] Palinginis KC, Cohen JD, Illie A, Conway NMJ, Milne WI. Defect band distributions in hydrogenated tetrahedral amorphous carbon / crystalline silicon. J Non Cryst Solids 2000; 1077: 266-9.

[18] Yalcin N, Sevnic V. Studies on silica obtained from rice husk. Ceram Int 2001; 27: 219-24.

[19] Solum MS, Pugmine RJ, Jagyoten M, Derbyshire F, Evolution of carbon structure in chemically activated wood. Carbon 1995; 33: 1247-54.

[20] Liou TH, Preparation and characterization of nanostructured silica from rice husk. Mater Sci Eng (in press)

[21] Stephen Trassl, Gunter Motz, Ernst Rossler, Gunter Ziegler. Characterizations of the free carbon phase in precursor derived SiCN ceramics. J Non Cryst Solids 2001; 293-5: 261-7.

[22] Kazuyoshi Kuriyama. Electronic properties of activated carbon fibers. The Sumitomo Search 1993; 52: 149-54.

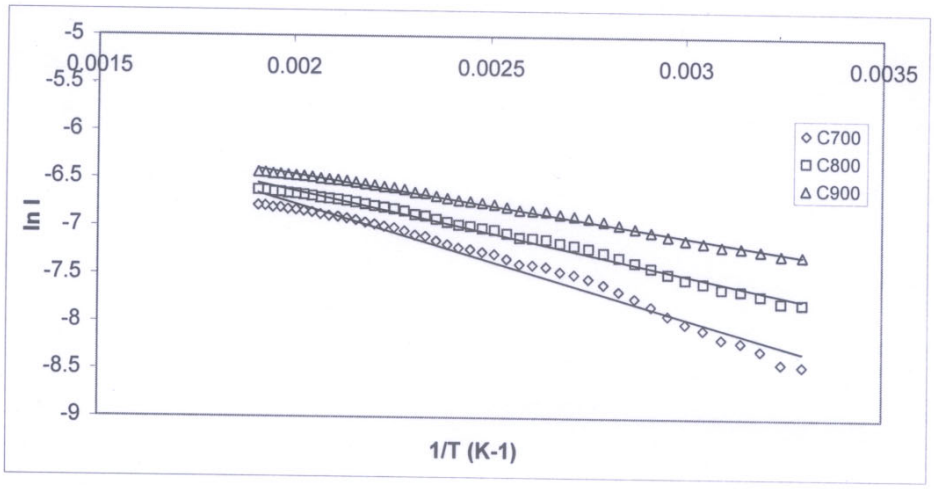

Fig. 1. Temperature dependence conductivity of different carbons measured from 30 to 250 C

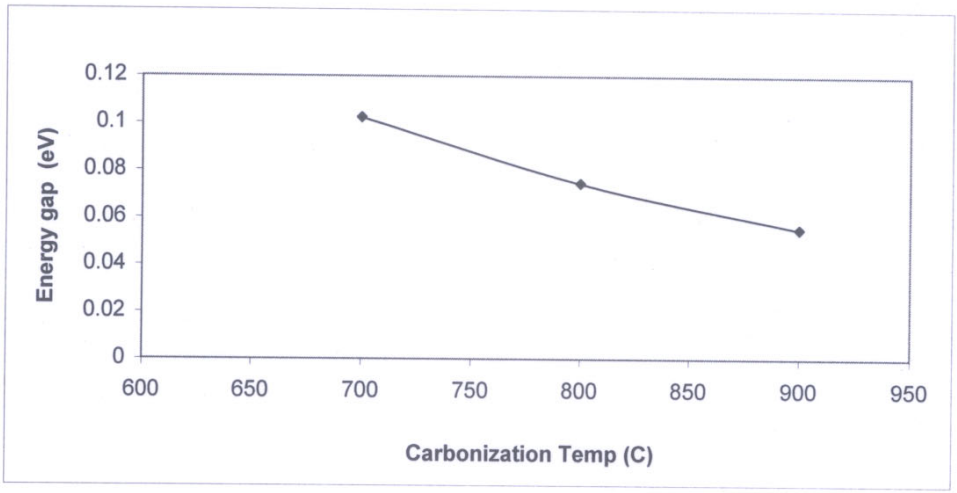

Fig. 2. Estimated energy gap for hopping conduction in carbon powders at different carbonization temperature

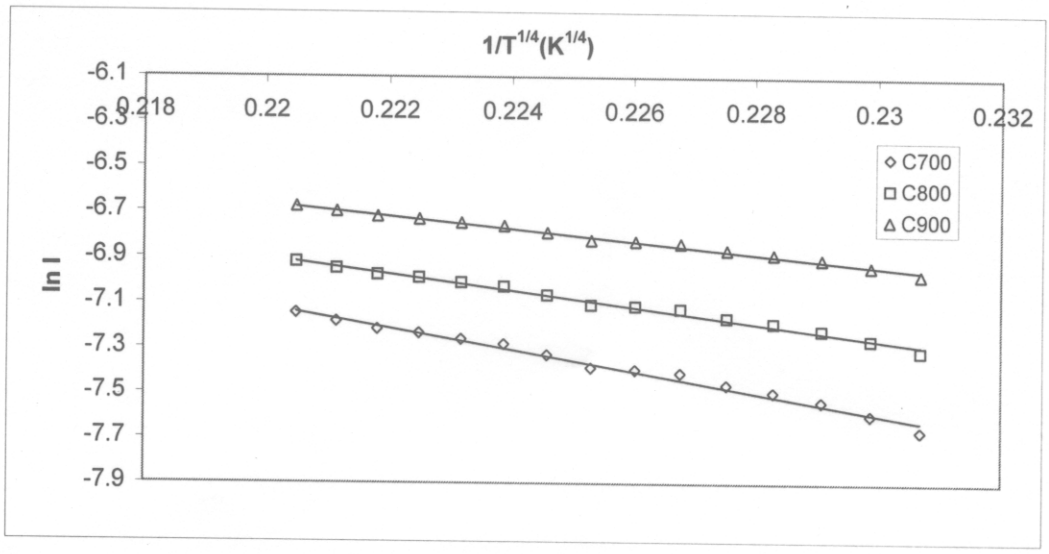

Fig. 3. Temperature dependence conductivity of different carbons measured from 80 to 150 C

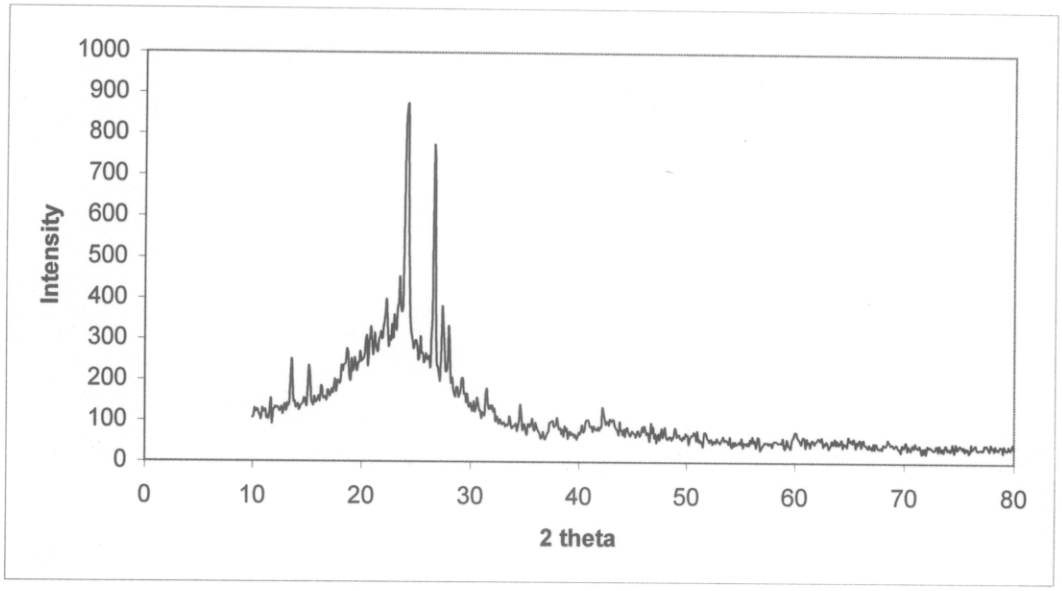

Fig. 4. X - ray diffaction curve of C900 sample

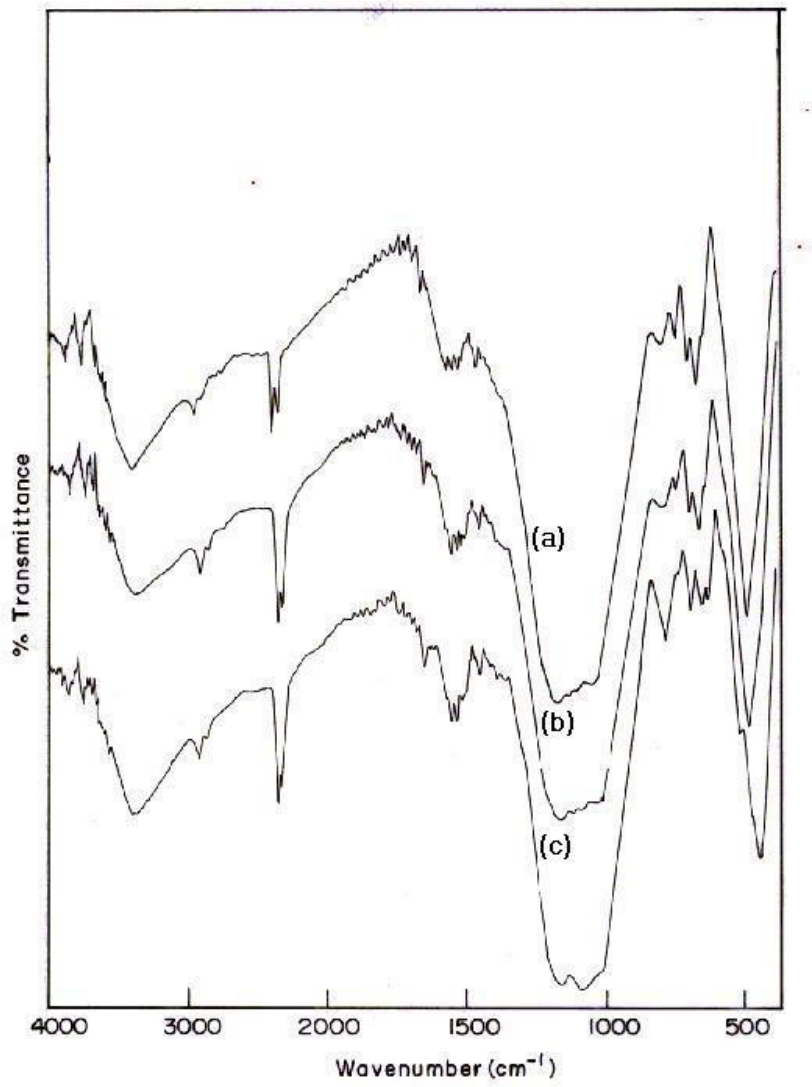
% Transmittance
(a)
(b)
(c)
4000
3000
2000
1500
1000
500
Wavenumber (cm⁻¹)

Figure 5.

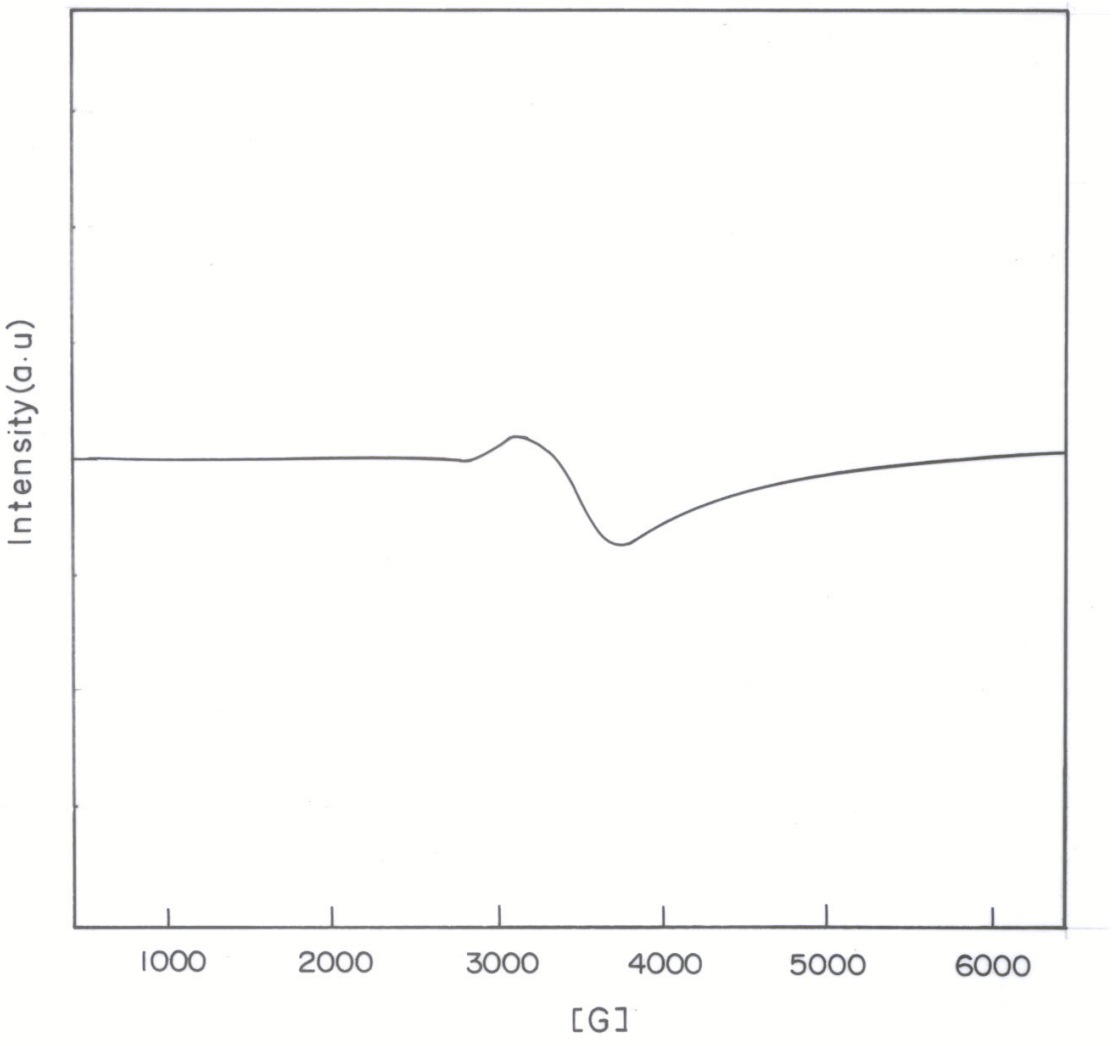

Fig. 6. Electron spin resonance spectra of C900 carbon sample.